Short Gamma Ray Bursts: The variability time scales in the Black Hole – Neutron Star Merger

Kostas Sapountzis [1] Agnieszka Janiuk[2]

[1,2]Center for Theoretical Physics Polish Academy of Science

[1]kostas@cft.edu.pl [2]agnes@cft.edu.pl

Introduction

The aim of the present work is to investigate the progenitors of the Short GRB characteristics in the framework of the Black Hole - Neutron Star merger (BH-NS). We used HARM *(Gammie et al 2003; Noble et al 2006)* a General Relativistic Magnetohydrodynamic code (GRMHD) that integrates the equations on a fixed Kerr spacetime to identify the implications of the NS magnetic field on the jet launching and determine the distance where the NS disruption takes place.

.

It is known that in both Short and Long GRBs a high Lorentz Factor of the emitting region is necessary to avoid the compactness problem. As a consequence the baryon load of the outflow must be low enough to obtain the requested acceleration *(Lei et al.2013)*. Another feauture of the prompt emission light curve is their intense variability with structures of $(10^{-4} - 10^{-2})$ *sec (MacLachlan et al 2013)*.

The radius where the tidal disruption of the companion NS takes place is an important quantity entering the initial conditions of our simulations. Much of work has been done in the last decade, but the results strongly depend on the NS equation of state and the BH spin parameter *(Ferrari et al 2010, Kumar et al 2017, Paschalidis 2017)*. For a highly rotating BH and a polytropic equation of state the suggested range is from few to few tenths Schwarchild radius.

Initial Set Up

The initial configuration consists of a Fishbone - Moncrief torus *(Fishbone & Moncrief 1976)* in orbit around a highly rotating Kerr Hole, $\alpha = 0.9$, with its innermost radius, r_{in}, and the radius where the maximum pressure occurs, r_{max}, in a range of values. Following *(Gammie et al 2003)* we use the geometrized system of units and the value of the torus maximum initial density, $\rho_{torus,in} = 1$, to scale the density all over the space of integration

$$r_g = \frac{GM}{c^2} = 1.48 \cdot 10^5 \frac{M}{M_\odot}\,\mathrm{cm} \qquad t_g = \frac{r_g}{c} = 4.9 \cdot 10^{-6} \frac{M}{M_\odot}\,\mathrm{sec} \qquad f_g = 6.0 \cdot 10^{20} \sqrt{\rho_{torus}} \left(\frac{M}{M_\odot}\right)^2 \mathrm{Mx}$$

where r_g, t_g, f_g the spatial, time and magnetic flux units respectively; the last scale is derived by the cgs definition of the magnetic units and the r_g, t_g, ρ_{torus} units assumed.

The magnetic field we impose is the field of a circular wire of radius $R = r_{max}$ *(Jackson1999)*

$$A_\varphi(r,\theta) = \frac{A_0}{\sqrt{r^2 + 2rR\sin\theta + R^2}} \frac{(2-k^2)K(k^2) - 2E(k^2)}{k^2} \qquad \text{where} \quad k = \sqrt{\frac{4Rr\sin\theta}{r^2 + R^2 + 2rR\sin\theta}}$$

and E,K the complete elliptic functions. The constant A_0 scales the magnetic field magnitude and it is used to set the plasma-β parameter on the torus; notice that this choice affects also the surrounding (ISM) plasma-β the density of which is much smaller than in the toroidal plasma.

A final implication of the magnetic field imposed is that the Fishbone - Moncrief torus is no longer on steady state. Nevertheless and as long as the β_{torus} is high, we can assume a steady state in a good approximation. In contrast the interstellar medium is a low density, cold and polytropic fluid threaded by the torus magnetic field. Due to its lower density the β_{ism} varies from higher values far away from the NS to much lower in its vicinity.

Among the parameters involved we select to investigate the implications of the magnetic field of the disrupted NS and of the distance were the disruption of the companion takes place. The values of the initial parameters imposed are shown in the table beside. The maximum allowed value of the Lorentz Factor was set at $\gamma_{max} = 50$ for all the models considered.

Model	FM torus radius r_g units r_{in}	r_{max}	ISM Density ρ_{torus} units	A_0 f_g units	Plasma - β torus	ism
HD-Therm	500	520	$4 \cdot 10^{-12}$	$2.3\,10^{-6}$	$5.3\,10^{18}$	$1.4\,10^{9}$
MD-Magn	100	120	$1.2\,10^{-10}$	1.0	$2.6\,10^{6}$	$6.5\,10^{-4}$
LD-Therm	10	12	$1.2\,10^{-8}$	$1.3\,10^{-8}$	$3.0\,10^{18}$	$3.9\,10^{10}$
LD-Magn	10	12	$5.1\,10^{-4}$	1.0	$2.6\,10^{-3}$	$2.6\,10^{-4}$

Table 1. The initial values of the models presented, see text for the quantities definition, see text for the units definition. The ρ_{ISM} is normalized to the toroidal maximum density.

Results

The first model, HD-Therm, refers to a torus at a high distance orbit and of negligible magnetization, *left column fig.1*. The accretion of the NS fluid and the frozen flux theorem leads to the formation of a magnetic barrier *(Bisnovatyi&Ruzmaikin 1976; McKinney et al 2014)* which increases the magnetic field magnitude and prevents baryons from entering this region. As a consequence an outflow of much lower parameter-β, but still thermally dominated, is being obtained, *middle column fig 1*.

The launching of the jet results to the formation of a relativistic inhomogeneous flow. For the specific integration time we obtain a single mutli-lorentz pulsation with peaking values $\gamma_{jet} \sim 3\text{-}12$, *right column fig 1*.

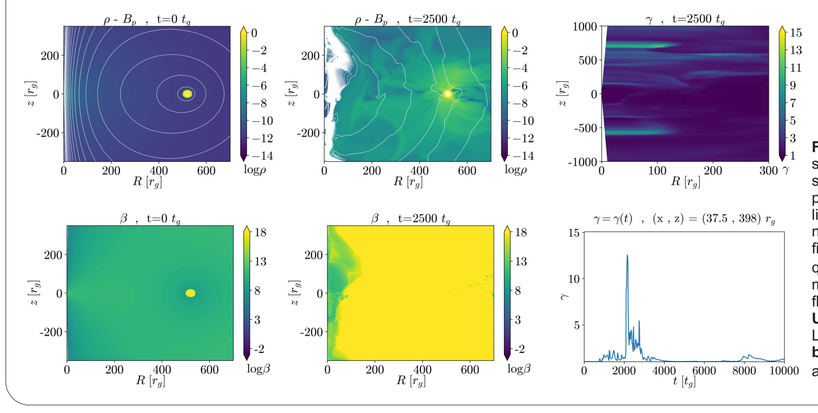

Fig 1. *HD-Therm* model. **Left column:** The color scale of the panels stands for the logarithmic spatial distribution of the density and the parameter-β at the initial conditions. The white lines corresponds to the magnetic field lines, notice the topology corresponding to the magnetic field of a circular wire. **Middle column:** The same quantities at $t = 2500\ t_g$. Notice the formation of the magnetic barrier and the increase of the magnetic flux, the outflow remains still thermally dominated. **Upper right panel:** The spatial distribution of the Lorentz Factor for a z-enlongated regime. **Right bottom panel:** The Lorentz Factor of the outflow at a specific point of the space $(x = 37.5\ ,\ z = 398)\ r_g$.

Results

The magnetic dominated model *MD-Magn* consists of a torus at $r_{max} = 120\ r_g$ and still of very high β-parameter, *left column fig 2*. The crucial difference of this model lays at the magnetic barrier formation which lead to a magnetic dominated jet, *middle column fig 2*.

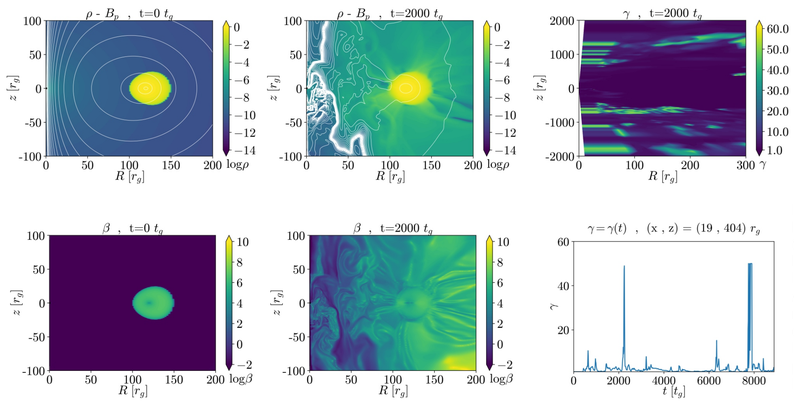

Fig 2. *MD-Magn* model. **Left column:** The logarithmic spatial distribution of the density and the parameter-β at the initial conditions. The solid lines of the corresponds to the magnetic field lines. **Middle column:** The same quantities at $t = 2000\ t_g$. The magnetic barrier leads to the formation of a magnetic dominated jet. **Upper right:** The spatial distribution of the γ for a z-enlongated regime. **Right bottom:** The Lorentz Factor at a specific point $(x = 19.0\ ,\ z = 404)\ r_g$. Notice the Lorentz Factor barrier and the variability time scale.

The resulting outflow constitutes of two inhomogeneous blobs with high Lorentz Factors close to the ones expected in GRBs, *right column fig 2*; the final values are restricted by the Lorentz Factor barrier. The variability time scale of the outflow is $\Delta t_{blobs} \sim 6000 t_g$.

The two models where the NS lays in a closer distance to the BH, *LD-Therm* and *LD-Mag*, appear in the *first* and *second row fig 3*. As in the previous cases the magnetic barrier formation leads to a higher magnetized jet, thermally or magnetically dominated respectively.

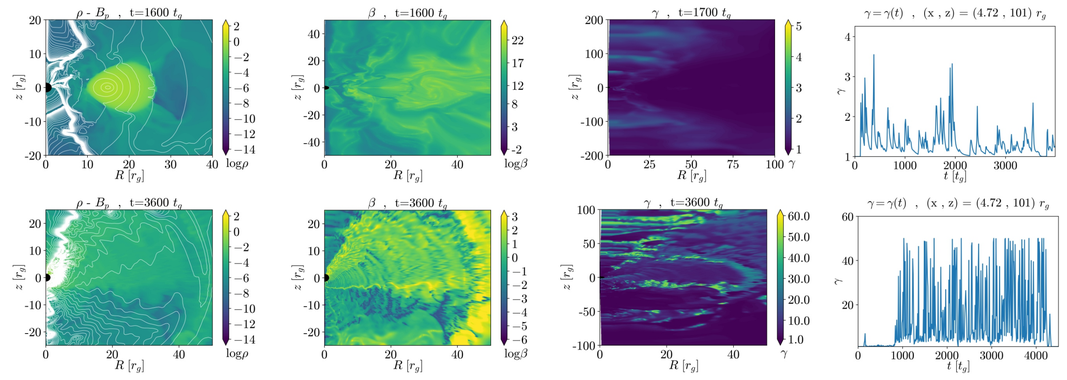

fig 3. The *LD-Therm* (upper row) and *LD-Magn* (bottom row). **1st and 2nd column:** The color scale stands for the logarithm of the density and parameter-β respectively, while the solid lines represent magnetic field lines. In both models we notice the magnetic barrier, but in the LD-Magn the torus has been deformed; nevertheless there is still enough material in the region to accrete and power the jet. **3rd column:** The spatial distribution of the Lorentz Factor where the multiple blobs in the jet exists. In the LD-Magn we notice also a wind outflow. **4th column:** The Lorentz Factor of the outflow at specific points. Both models present great variability, but the *LD-Magn one concludes also in high Lorentz Factors.*

The resulting outflow is constituted by multiple blobs, *third* and *fourth column fig 4*, with typical time variability $\Delta t_{blobs} \sim 300\ t_g$ and $\Delta t_{blobs} < 200\ t_g$ respectively. The Lorentz Factor achieved in the magnetically dominated outflow is much higher and more appropriate for the Short GRB phenomenon. A crucial difference in the magnetically dominated model in such a close to the BH distance is the fast deformation and kick of the initial torus due to the interaction with the accreting and ISM material that doesn't accrete. Nevertheless, there is enough material left to power the jet launching and highly accelerated blobs.

Conclusions

We performed a parametrical study based on the position of the torus and the initial magnetic field magnitude using as criterion the acceleration and the inhomogeneous structures of the launched jet. In the models we present the initial low magnetization and the magnetic field accretion results to a magnetic barrier formation which prevents the baryon loading in the jet region, enhances the magnetic field magnitude and leads to a higher magnetized outflow.

The time scale of the jet variability crucially depends on the initial position of the torus, i.e. at the radius where the tidal disruption takes place. Our findings are in accordance-argue in favor of the dominant modeling where the tidal disruption takes place at few, to very few tenths of r_g. The variability of *LD-Therm*, *LD-Magn* models assuming a $3M_\odot$ BH yields $\Delta t_{blobs} \sim 4.4 \cdot 10^{-3}$ *sec* and $\Delta t_{blobs} < 2{,}9 \cdot 10^{-3}$ *sec*, while of *MD-Magn,* $\Delta t_{blobs} \sim 8.8 \cdot 10^{-2}$ *sec*, is high for the SGRB.

The magnetization of the initial torus is crucial for the acceleration of the launched jet through the magnetic barrier enhancement. In all the models presented and run the lower parameter-β leads to higher Lorentz Factors. Nevertheless, higher initial β_{torus} values result the torus deformation and some special assumptions of theISM like increased density which have to be further investigated. This is the topic where our current research is focused on.

References

- Bisnovatyi-Kogan G.S., Ruzmaikin A.A., 1976, Ap&SS, 42, 401B
- Ferrari F.V., Gualtieri L., Pannarale F., 2010,PhysRevD, 81, 064026
- Fishbone L.G., Moncrief V., 1976, 207, 962
- Gammie C.F, McKinney J.C.,Toth G. 2003, ApJ, 589, 444
- Jackson J.D., "Classical Electrodynamics", Third Edition, 1999, NY Wiley
- Kumar P.,Pürrer M., Pfeiffer H.P., 2017, PhysRevD, 95, 044039
- Lei W.H., Zhang B., Liang E.W. 2013, ApJ, 765, 125
- MacLachlan G.A. et al, 2013, MNRAS, 432, 857
- McKinney J.C., Tchekhovskoy A., Blandford R.D., 2014, MNRAS, 423, 3083
- Noble S.C., Gamie C.F., McKinney J.C., 2006, 641, 626
- Pachalidis V., 2017, Class. Quantum Grav., 34, 084002

Acknowledgment

This research was supported in part by grant DEC-2012/05/E/ST9/03914 from the Polish National Science Center. We also acknowledge support from the Interdisciplinary Center for Mathematical Modeling of the Warsaw University, through the computational grants G53-5 and gb66-3.